




Hyperbiofilm Formation by *Bordetella pertussis* Strains Correlates with Enhanced Virulence Traits

Natalia Cattelan,^a Jamie Jennings-Gee,^b Purnima Dubey,^{c,d}
 Osvaldo M. Yantorno,^a Rajendar Deora^{b,d}

Centro de Investigación y Desarrollo en Fermentaciones Industriales (CONICET, CCT-La Plata), Facultad de Ciencias Exactas, Universidad Nacional de La Plata, La Plata, Argentina^a; Department of Microbiology and Immunology^b and Department of Pathology,^c Wake Forest School of Medicine, Winston-Salem, North Carolina, USA; Department of Microbial Infection and Immunity, The Ohio State University Wexner Medical Center, Columbus, Ohio, USA^d

ABSTRACT Pertussis, or whooping cough, caused by the obligate human pathogen *Bordetella pertussis* is undergoing a worldwide resurgence. The majority of studies of this pathogen are conducted with laboratory-adapted strains which may not be representative of the species as a whole. Biofilm formation by *B. pertussis* plays an important role in pathogenesis. We conducted a side-by-side comparison of the biofilm-forming abilities of the prototype laboratory strains and the currently circulating isolates from two countries with different vaccination programs. Compared to the reference strain, all strains examined herein formed biofilms at high levels. Biofilm structural analyses revealed country-specific differences, with strains from the United States forming more structured biofilms. Bacterial hyperaggregation and reciprocal expression of biofilm-promoting and -inhibitory factors were observed in clinical isolates. An association of increased biofilm formation with augmented epithelial cell adhesion and higher levels of bacterial colonization in the mouse nose and trachea was detected. To our knowledge, this work links for the first time increased biofilm formation in bacteria with a colonization advantage in an animal model. We propose that the enhanced biofilm-forming capacity of currently circulating strains contributes to their persistence, transmission, and continued circulation.

KEYWORDS *Bordetella pertussis*, biofilms, hyperbiofilm, virulence

Bordetella pertussis is a human-restricted bacterial pathogen that causes whooping cough, or pertussis. Pertussis has been reemerging in industrialized countries and remains endemic in many parts of the world (1). Current pertussis vaccines, while preventing the severe symptoms of the disease, do not prevent colonization, transmission, and circulation of the pathogen (2). Reasons suggested for the reemergence of pertussis are (i) heightened disease awareness, (ii) development of new clinical definitions, (iii) improved diagnostic ability, (iv) poor efficacy of the current commercial vaccines, and (v) antigenic and genetic shifts in circulating strains (3).

Genetic changes in currently circulating strains of *B. pertussis* have been primarily observed in genes which encode vaccine antigens, such as pertussis toxin (PT), filamentous hemagglutinin (FHA), pertactin (PRN), and fimbriae (Fim2 and Fim3) (4–8). In addition, isolates deficient in the production of PRN, FHA, and PT (9–11) and those showing increased production of PT have also been reported (12). These genetic and phenotypic alterations are hypothesized to confer an adaptive advantage to the circulating strains with respect to survival and transmission among vaccinated populations (12, 13). Based on these assumptions, it is proposed that the laboratory reference strains, after more than 6 decades of *in vitro* passage, do not represent the circulating *B.*

Received 24 May 2017 Returned for
modification 26 June 2017 Accepted 3
September 2017

Accepted manuscript posted online 11
September 2017

Citation Cattelan N, Jennings-Gee J, Dubey P,
Yantorno OM, Deora R. 2017. Hyperbiofilm
formation by *Bordetella pertussis* strains
correlates with enhanced virulence traits. Infect
Immun 85:e00373-17. <https://doi.org/10.1128/IAI.00373-17>.

Editor Andreas J. Bäuml, University of
California, Davis

Copyright © 2017 American Society for
Microbiology. All Rights Reserved.

Address correspondence to Osvaldo M.
Yantorno, yantorno@quimica.unlp.edu.ar, or
Rajendar Deora, rajendar.deora@osumc.edu.
O.M.Y. and R.D. contributed equally to this
article and jointly supervised the work.

pertussis organisms (14). This accentuates the need for research on recently circulating strains with respect not only to uncovering genomic alterations but also to understanding phenotypic variations, an area that remains poorly studied.

Biofilms are sessile microbial communities which are enclosed in a self-produced or host-derived exopolymeric matrix (15). In some bacteria, biofilms promote environmental survival, resulting in an enhanced probability of host contact, while in others, biofilms are a critical virulence determinant (16, 17). Many bacteria form biofilms during infection of nonmammalian and mammalian hosts, and biofilms are in general less susceptible to antimicrobials and host immune components (18–20). Biofilms of *B. pertussis* have been observed on a variety of artificial surfaces and under static, shaking, and fluid flow conditions (21–25). Microscopically, *B. pertussis* biofilms are characterized by formation of spaced cell aggregates followed by the formation of three-dimensional structures (pillars of bacteria separated by fluid channels or irregularly shaped microcolonies) encased in an opaque matrix composed of DNA and polysaccharide (23–27). In addition to their presence in laboratory settings, biofilms of *B. pertussis* bacteria have also been detected in the nose and trachea during experimental infections of mice (24, 25, 27). Correlation between the biofilm-forming ability of *B. pertussis* and pathogenesis is provided by the finding that mutants defective in biofilm formation on artificial surfaces fail to protect the bacterial cells from complement-mediated killing, are attenuated for colonization of the mouse respiratory tract, and are defective in biofilm formation on the respiratory tract (24, 27, 28). This has led to the hypothesis that biofilm formation in humans enables escape from immune defenses, resulting in persistence, transmission, and continued circulation of the bacteria (29). Support for this hypothesis is provided by microscopy of human tissue explants and respiratory tissues of patients that reveal biofilm-like structures similar to those formed on artificial surfaces and in mouse organs (30–32).

Very little is known about the mechanisms by which *B. pertussis* biofilm growth has adapted with respect to time, region, and changing immunization regimens. While increased levels of biofilm formation by circulating strains from Argentina and Australia have been reported (33, 34), nothing is known about the biofilm-forming abilities of circulating isolates from the United States. It is also not known if there are differences in biofilm structures between strains from different countries. In this report, we performed a side-by-side comparison of the biofilm-forming abilities of currently circulating strains from the United States and Argentina with the objective of determining variations in biofilm-forming capacities and structures. We have also examined the mechanistic bases for hyperbiofilm formation. Finally, we have investigated the relationship between enhanced biofilm formation and pathogenic phenotypes.

RESULTS

Recently circulating strains of *B. pertussis* from the United States and Argentina form a thick bacterial ring at the air-liquid interface and display a hyperbiofilm phenotype. The biofilm-forming abilities of *B. pertussis* strains currently circulating in the United States are not known. During routine roller drum growth in glass tubes of one such strain (STO1-SEAT0004), we noticed a thick bacterial ring at the liquid-air interface. In comparison, the reference laboratory strains *B. pertussis* Tohama I and Bp536, a Tohama I derivative, formed either a thinner ring or did not form a ring (Fig. 1A). We followed this observation with additional strains from the United States and Argentina and grew them side by side for comparison purposes. The U.S. strains resulted in either compact rings at the air-liquid interface or diffused rings over the glass surface. For the strains that formed diffused rings (strains H973, S49560, and H897), very little bacterial growth was visible in the liquid phase (Fig. 1A). In comparison, all the Argentinean strains formed compact rings at the air-liquid interface.

We have previously reported a link between the formation of a ring at the air-liquid interface and biofilm formation in RB50, a *Bordetella bronchiseptica* reference strain (35). Additionally, a cystic fibrosis isolate of *B. bronchiseptica* which formed a thicker ring than RB50 formed biofilms at higher levels (36). Thus, we hypothesized that recent

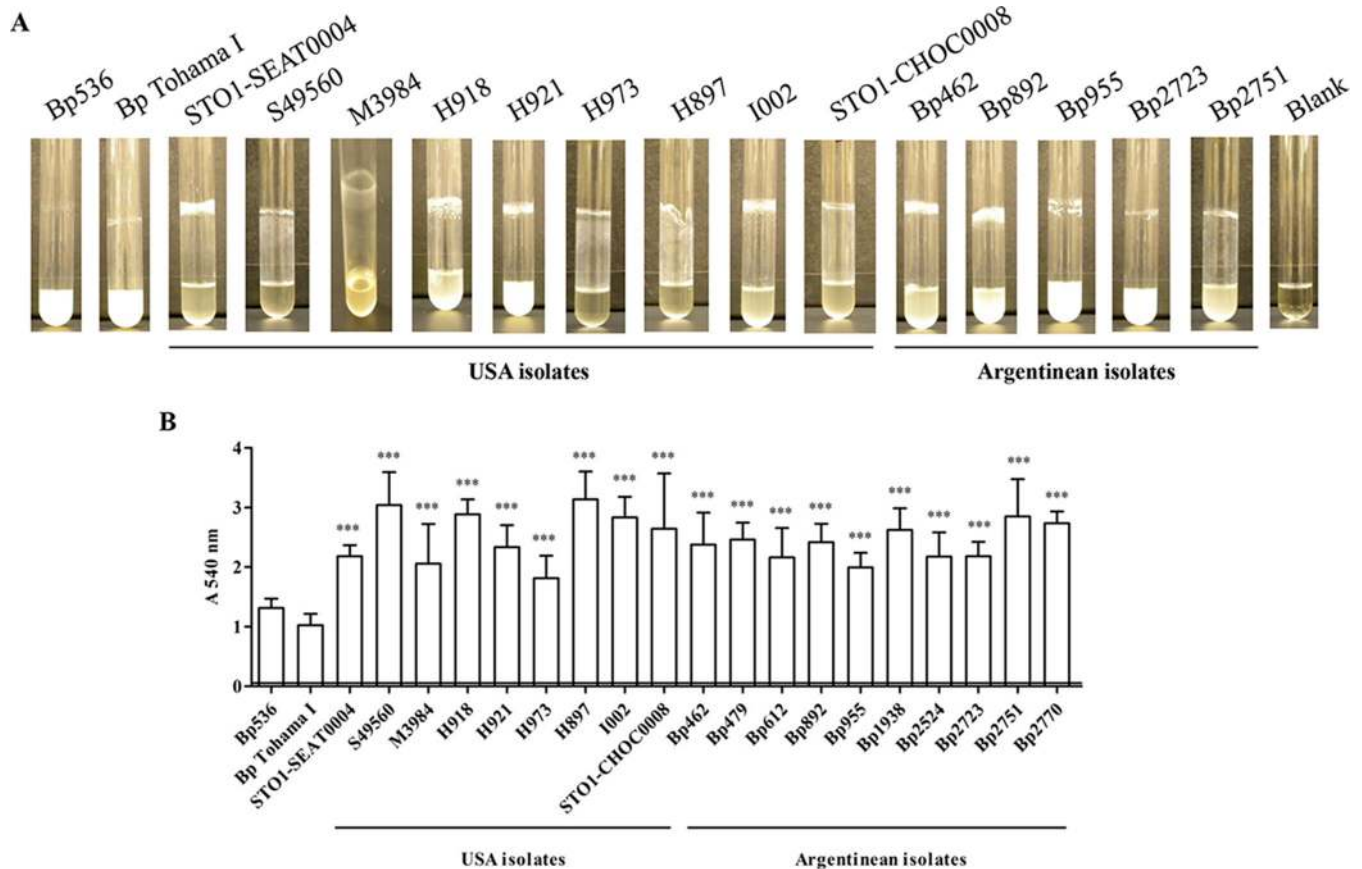


FIG 1 Biofilm-forming capacity of *B. pertussis* strains. (A) Formation of a bacterial ring at the air-liquid interface of glass culture tubes. (B) Microtiter assay of biofilm formation at 96 h by *B. pertussis* strains. Each data point represents the average value of three independent experiments performed in quadruplicates; error bars indicate standard deviations. Significant differences were assessed by one-way ANOVA and Bonferroni posttest. ***, $P < 0.001$.

isolates of *B. pertussis* possess a hyperbiofilm phenotype. To test this hypothesis, we quantified biofilms formed on polystyrene microtiter plates. After bacteria from the planktonic phase were discarded and the plates were subjected to extensive washing, the attached biomass was quantified by staining adhered bacteria with crystal violet (CV).

In comparison to Bp536 and BpTohama I, all recent isolates formed high levels of biofilms on microtiter plates (Fig. 1C). The observed differences in biofilm levels cannot be explained by enhanced growth since none of the recent isolates displayed significantly higher growth than Bp536 in the planktonic phase of biofilm cultures (data not shown). In combination, these results suggest that recently circulating strains of *B. pertussis* form higher levels of biofilms than the model laboratory-adapted strains.

Hyperbiofilm-forming strains display hyperaggregative properties. Very little is known about the mechanisms that contribute to hyperbiofilm formation in *B. pertussis*. A positive correlation between autoaggregation and biofilm formation has been reported in bacteria (36, 37). We compared the autoaggregation index (AI) of three randomly chosen recently circulating strains from Argentina (Bp462, Bp892, and Bp2751) and the United States (H921, H973, and STO1-SEAT0004) with that of Bp536 (Fig. 2). AI represents the fraction of cells that aggregated (relative to the total cell population). After 2 h of static incubation, the AI of each of these six strains was 8- to 16-fold higher than that of Bp536. To determine the kinetics of cellular aggregation, the culture tubes were additionally incubated statically for 5 and 24 h. While at 5 and 24 h of incubation the AI of Bp536 was higher than that at 2 h, it never reached the values observed for the clinical strains. For the clinical strains, there was not a significant increase in the AI at 5 and 24 h compared to that at 2 h. We conclude that the clinical

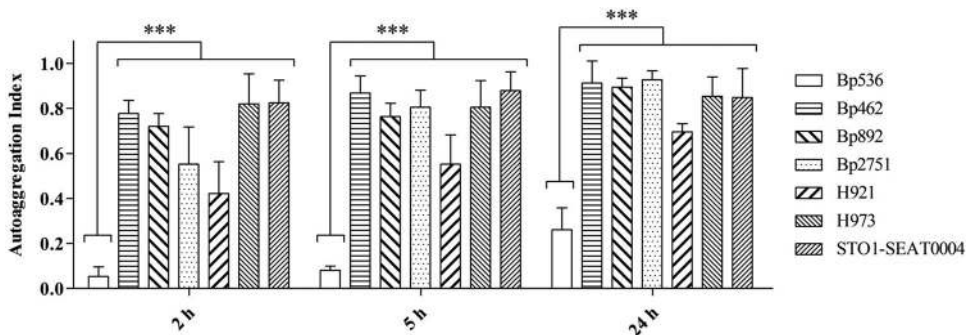


FIG 2 Quantification of autoaggregation of *B. pertussis* strains. Each bar represents the mean value of at least three independent experiments performed in duplicate. Error bars represent standard deviations. Statistical differences were assessed by one-way ANOVA and Bonferroni posttest. ***, $P < 0.001$.

strains form cellular aggregates faster and at higher levels than the reference strain. These results suggest that the clinical strains utilize hyperaggregation as a means to enhance their biofilm-forming capacities.

Recently isolated strains of *B. pertussis* display increased aggregation during initial surface attachment and form biofilms with enhanced structural complexity.

The approaches used above do not provide detailed information on either the qualitative or quantitative strain-specific differences in biofilm structures. The objective of the next experiment was to conduct *in situ* visualization and analyses of differences in the biofilm three-dimensional (3D) architecture of these strains. For this purpose, each of the six recently circulating strains and Bp536 were transformed with a green fluorescent protein (GFP)-coding plasmid, followed by culture on glass coverslips under agitation conditions, and initial attachment and the biofilms formed were compared.

We first examined differences in initial attachment by incubating the strains on the substrate for 1 h, followed by microscopic observation. As shown in Fig. 3A, all six recently isolated strains adhered to the surface by forming aggregates, which were largely absent from Bp536. The formation of small clusters by these strains is consistent with their higher AI values. Quantification of bacteria attached to the glass coverslips revealed similar numbers of cells for all of the strains, including Bp536 (Fig. 3B). This suggests that the manner in which recently isolated strains attach to the surface is different from that of Bp536.

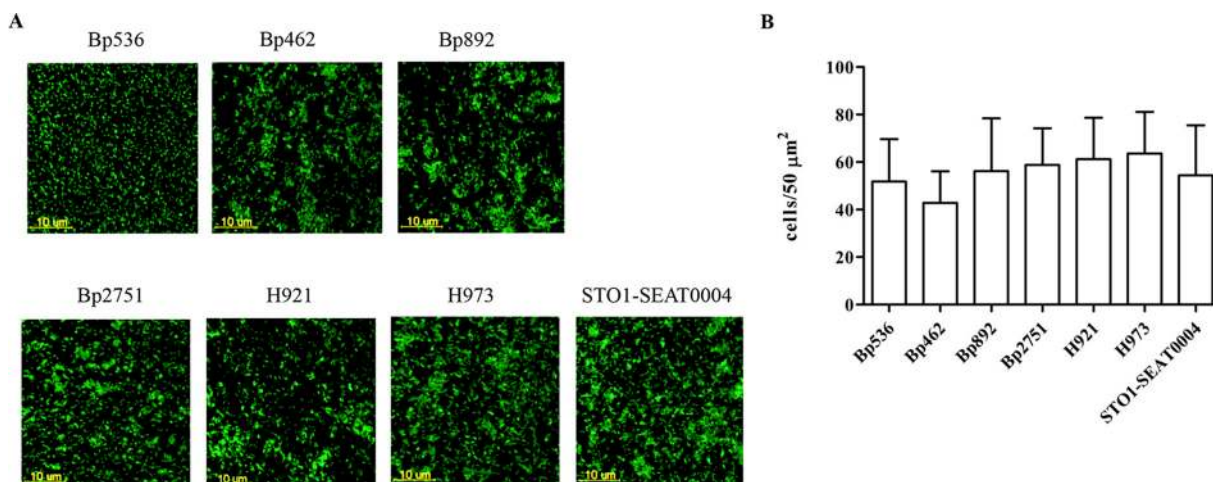


FIG 3 Fluorescence microscopy and quantification of early bacterial attachment. (A) Attached GFP-labeled bacterial cells were observed by fluorescence microscopy. (B) Cells were counted by means of the ITCN plug-in for ImageJ. Data are average values of at least three independent experiments performed in duplicates. Four random regions were chosen for bacterial counting. Error bars indicate standard deviations.

To observe and quantify the 3D structures of biofilms, the growth of biofilms was examined by confocal laser scanning microscopy (CLSM) at 24-h intervals over a time period of 96 h (Fig. 4). After 24 h of growth of Bp536, almost the entire surface area was completely covered with green cells which appeared to exist as a uniform monolayer. In contrast, all six recently isolated strains were present on the cover glass surface in the form of clustered cells, and many areas of the cover glass were observed to be unoccupied. For these strains, small pillars of cells, a characteristic architectural feature of *Bordetella* biofilms, were also found (23, 27). At 48 h of growth, while minute cell clusters and thin pillars were observed for Bp536, the recently isolated strains continued to increase in thickness and cell density, resulting in the visualization of thicker and more structured biofilms. After 72 and 96 h of culture, while Bp536 achieved a more complex biofilm structure involving the formation of some water channels, the recently isolated strains continued to form complex biofilm structures with large and irregularly shaped clusters and longer cell pillars.

Interestingly, in addition to structural differences, region-specific variations in the biofilm features were also observed among the recently isolated strains. At time points later than 24 h, for the strains isolated in the United States (H921, H973, and STO1-SEAT0004), large and irregularly shaped cell aggregates continued to be observed during the entire time course of biofilm formation, whereas for the Argentinean strains (Bp462, Bp892, and Bp2751) almost the entire surface area was green, revealing a thick uniform layer of cells.

Quantitative analysis of biofilm architecture. In order to achieve a quantitative assessment of the observed microscopic differences in biofilm structures, CLSM-generated images were analyzed for four variables of biofilm architecture—biomass, maximum thickness, average thickness, and roughness coefficient—by the COMSTAT2 image analysis program (Fig. 5) (38). Overall, and at all time points of biofilm formation, maximum thickness and average thickness were significantly higher for the recently isolated strains than for Bp536. The only exception was Bp892, for which the maximum biofilm thickness was not significantly different from that of Bp536 at 24 h. Biomass was significantly higher for all clinical isolates at 96 h. The roughness coefficient, a measure of how much the biofilm thickness varies and thus a measure of biofilm heterogeneity, varied the greatest between Bp536 and the clinical strains. In general, for the Argentinean strains, the roughness coefficient was lower than that of Bp536, whereas for the U.S. strains it was higher at many of the time points. The difference in roughness coefficients between the Argentinean and U.S. strains correlated with microcolonies separated by empty spaces, as observed by CLSM. Overall, these results suggest that the *B. pertussis* clinical strains form biofilms differently than the reference strain and that differences in biofilm structures are observed between strains isolated from United States and Argentina.

Dispersal of biofilms by pronase E, DNase I, and sodium metaperiodate. Previously, we have shown that proteins, DNA, and polysaccharides are components of the *B. pertussis* biofilm matrix and promote the stability of biofilms formed by Bp536 (21, 23–25). To address the functional roles of these components in stabilizing the biofilms of the recently isolated strains, we studied the effect of pronase E, DNase I, and sodium metaperiodate (NaIO_4) on dispersal of preformed mature biofilms. Ninety-six-hour-old biofilms were incubated either with these reagents or with the respective buffer solutions for 2 h at 37°C, followed by CV staining to quantitate the stained biomass. Compared to Bp536, for five of the six recently isolated strains, pronase E treatment led to low levels of biofilm dispersal (50.3% for Bp536 and varying between 25.3 and 32.3% for Bp462, Bp2751, H921, H973, and STO1-SEAT0004). For strain Bp892, however, pronase E treatment was sufficient to disperse the biofilms to levels similar to those observed for Bp536 (Fig. 6A).

Sodium metaperiodate treatment resulted in two different levels of biofilm dispersal. For three of the recently isolated strains (Bp462, Bp2751, and H921), dispersion of biofilms was similar to that observed for Bp536 (varying between 31.7 and 37.6%). For

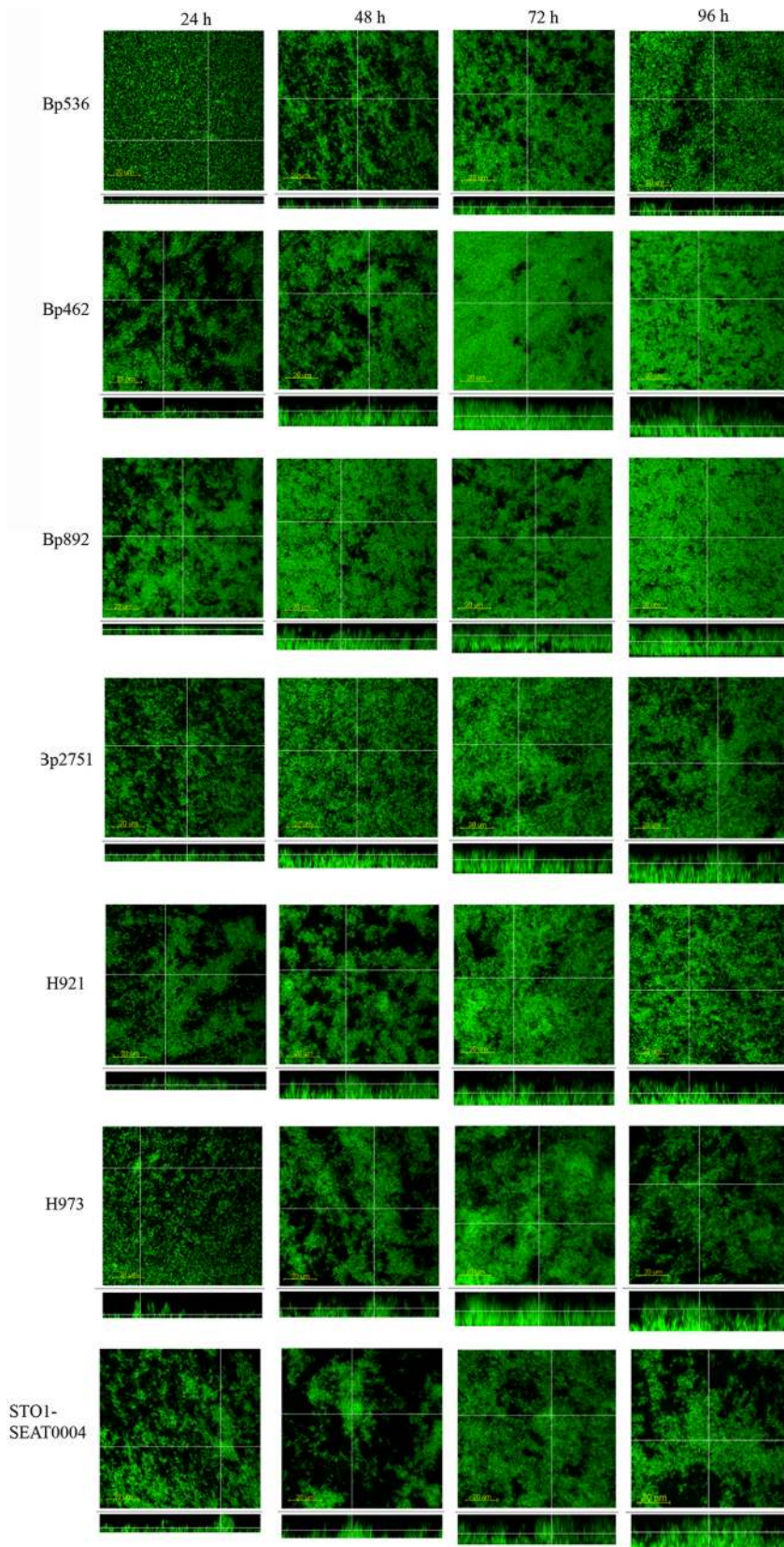


FIG 4 CLSM micrographs of *B. pertussis* biofilms. GFP-labeled bacterial strains were grown on cover glasses in six-well plates for the designated time points. Biofilms were visualized *in situ* by CLSM microscopy. CLSM image stacks were acquired at 0.9-μm z-intervals; xy and xz representative focal planes are shown.

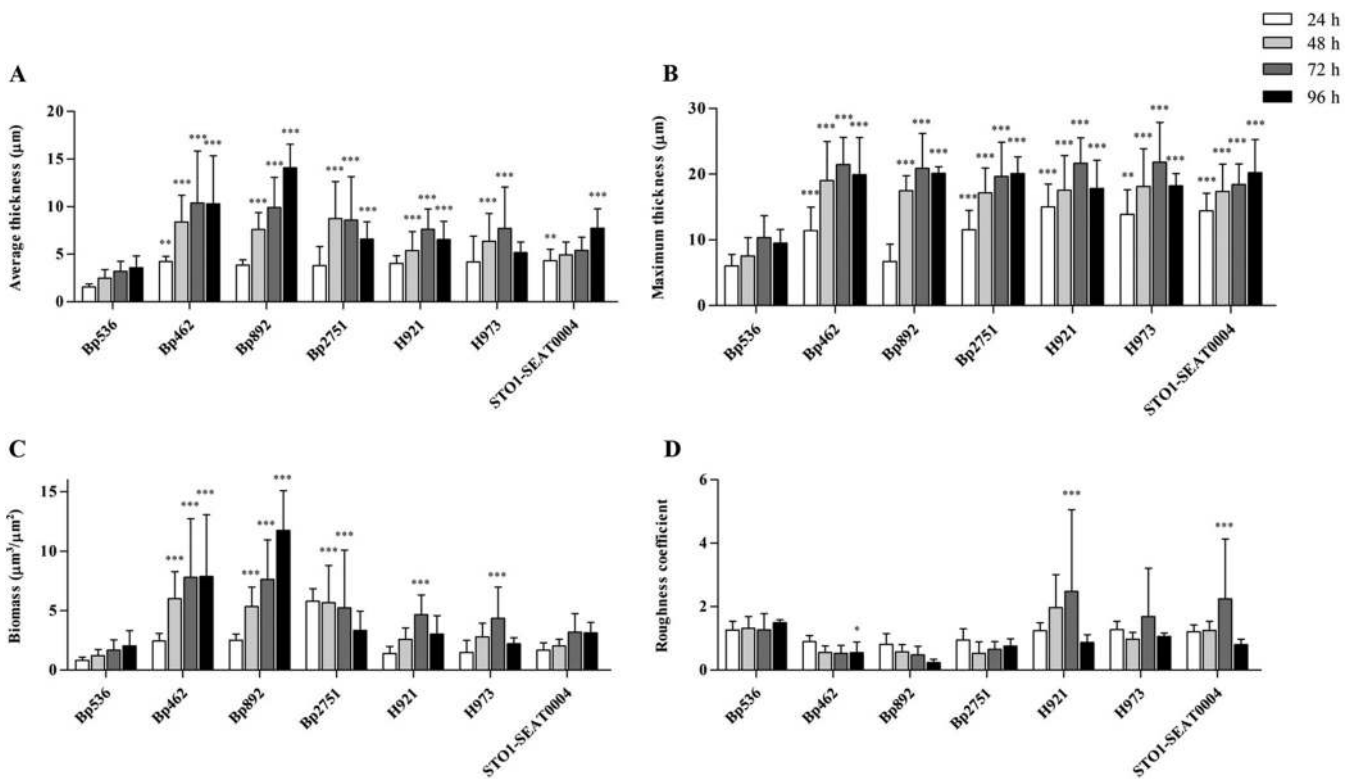


FIG 5 COMSTAT analyses of *B. pertussis* biofilms. CLSM image stacks were acquired at 0.9- μm z-intervals and analyzed by COMSTAT2. Average values of parameters from CLSM image stacks derived from at least three independent experiments are shown with standard errors. *P* values were determined using two-way ANOVA. Average thickness (A) and maximum thickness (B) were calculated only on the biomass (without counting the uncovered area). Biomass values (C) represent the biomass volume divided by the area of the substratum. Roughness coefficients (D) represent the variability in the heights of the biofilms. *, *P* < 0.05; **, *P* < 0.01; ***, *P* < 0.001.

the other three strains (Bp892, H973, and STO1-SEAT0004), however, NaIO_4 treatment resulted in significantly higher levels (varying between 60.4 and 66.9%) of biofilm dispersal (Fig. 6B).

Similar to results for Bp536, for four of the recently isolated strains (Bp892, Bp2751, H973, and STO1-SEAT0004), greater than 50% of biofilms were dispersed by treatment with DNase I. For Bp892, incubation with DNase I led to greater than 85% dispersal. For two of the isolates (Bp2751 and Bp462), DNase I had a somewhat moderate effect (35.4 and 40%, respectively) on biofilm dispersal (Fig. 6C). The various levels of biofilm dispersal as a result of incubation with the above chemicals are probably due to differences in biofilm formation between various strains. Taken together, these results suggest that, similar to Bp536, recently isolated strains have protein, DNA, and carbohydrate content in their biofilm matrices.

Recently isolated strains exhibit differential expression of *Bordetella* factors involved in biofilm formation and pathogenesis. Critical among factors that contribute to robust biofilm formation in *B. pertussis* are FHA, adenylate cyclase (AC) toxin, and Bps polysaccharide (24, 27, 39). FHA and AC toxin promote and inhibit *B. pertussis* biofilm formation, respectively (24, 39). Bps is critical for the stability and maintenance of the three-dimensional structure of *B. pertussis* biofilms (27). In addition to their roles in biofilm formation, FHA, AC toxin, and Bps also function as critical virulence factors for *B. pertussis* (27, 28, 40–42). Thus, we quantitated the expression levels of these factors in the clinical strains. As a negative control, the Δbvg^- phase-locked and the Δbps strains were used. These strains do not express FHA or AC toxin and Bps, respectively.

We performed a whole-cell enzyme-linked immunosorbent assay (ELISA) to determine the levels of cell surface-associated FHA. As shown in Fig. 7A, all of the recently isolated strains produced significantly larger amounts (between 2.6- and

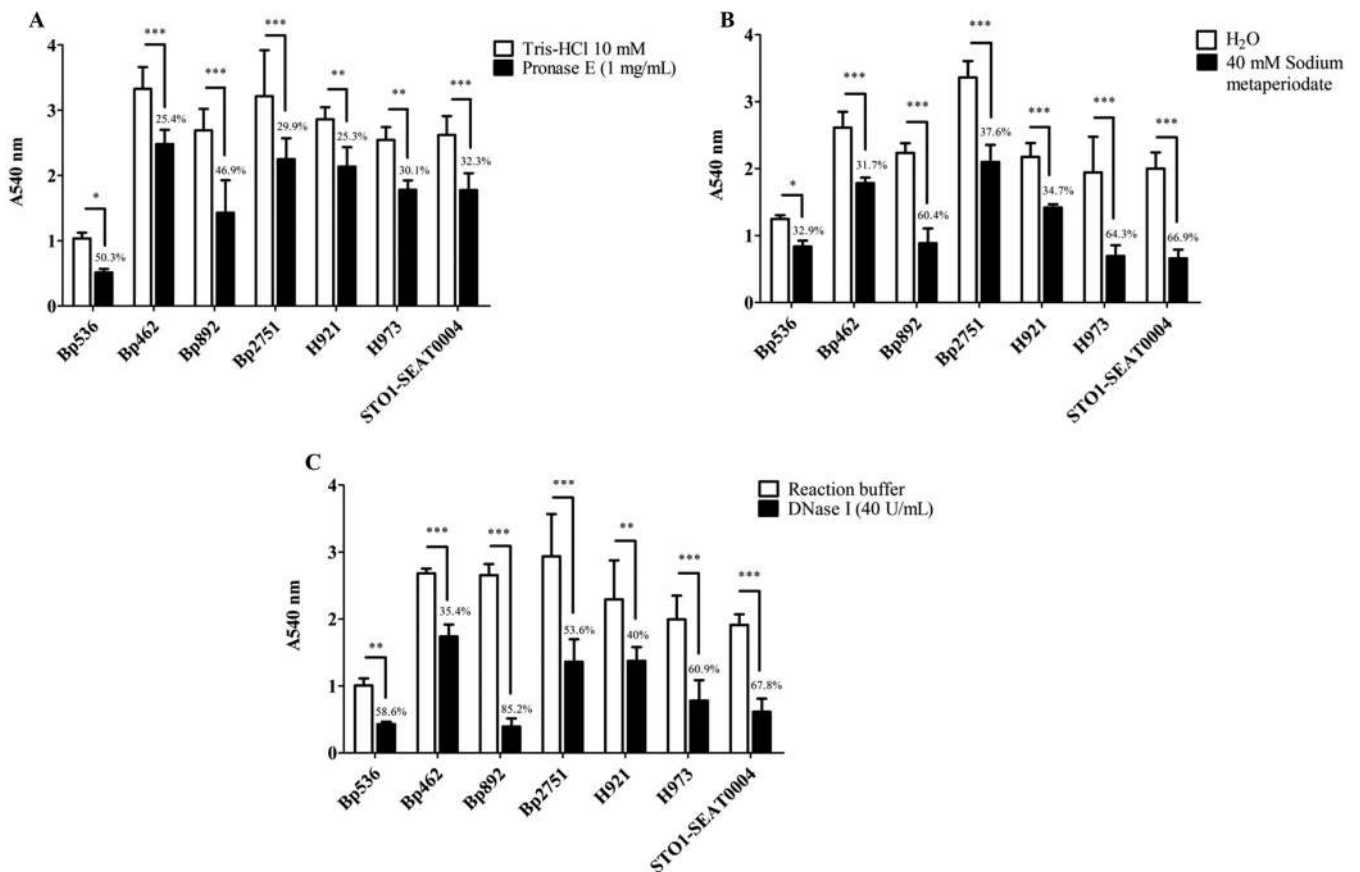


FIG 6 Biofilm dispersal by matrix-dissolving agents. Ninety-six-hour biofilms were treated with pronase E in Tris buffer (A), with 40 mM sodium metaperiodate (NaIO_4) in H_2O (B), and with DNase I in reaction buffer (C) for 2 h at 37°C (filled bars). Biofilms were treated with the respective reaction buffers as controls (open bars). Biofilm reduction is presented as a percentage of the value for the respective strain incubated with buffer only. Average values are shown from one representative assay of three independent replicates, with their respective standard deviations. Significance was assessed by two-way ANOVA. *, $P < 0.05$; **, $P < 0.01$; ***, $P < 0.001$.

3.3-fold) of FHA than Bp536. The expression of FHA was at background levels in this strain. As shown in Fig. 7B, all recent isolates displayed lower AC toxin activity than Bp536.

Changes in the expression of the *bps* locus were determined by quantitative reverse-transcription PCR (qRT-PCR) by comparing levels of the *bpsA* transcripts in Bp536 and the recently circulating strains. In two of the six recently isolates, expression of *bpsA* was significantly higher (5.4- and 1.6-fold higher in H921 and H973, respectively) (Fig. 7C). In four other strains, there were no significant differences in the expression levels of *bpsA* transcript. Bps production was detected by immunoblotting in all of the recently isolated strains (Fig. 7D). Using an ELISA, we failed to precisely and reproducibly quantitate Bps levels in the recently circulating isolates. Taken together, these results suggest that hyperbiofilm formation in recently isolated strains is associated with increased expression of genes/proteins that promote biofilm formation and decreased activity of the protein that inhibits biofilm formation.

Recently isolated strains exhibit hyperadhesion to respiratory epithelial cells of human origin. The recently isolated strains attached and formed higher levels of biofilms on artificial surfaces. Additionally, FHA was produced at higher levels in the clinical strains. FHA promotes the adherence of *B. pertussis* to epithelial cells (43). We hypothesized that, compared to Bp536, the recently circulating strains will exhibit increased cellular adherence to epithelial cells. To test this hypothesis, we compared attachment levels of these strains to human alveolar epithelial cells (A549). As shown in Fig. 8, all of the recently isolated strains adhered to A549 cells to a greater extent

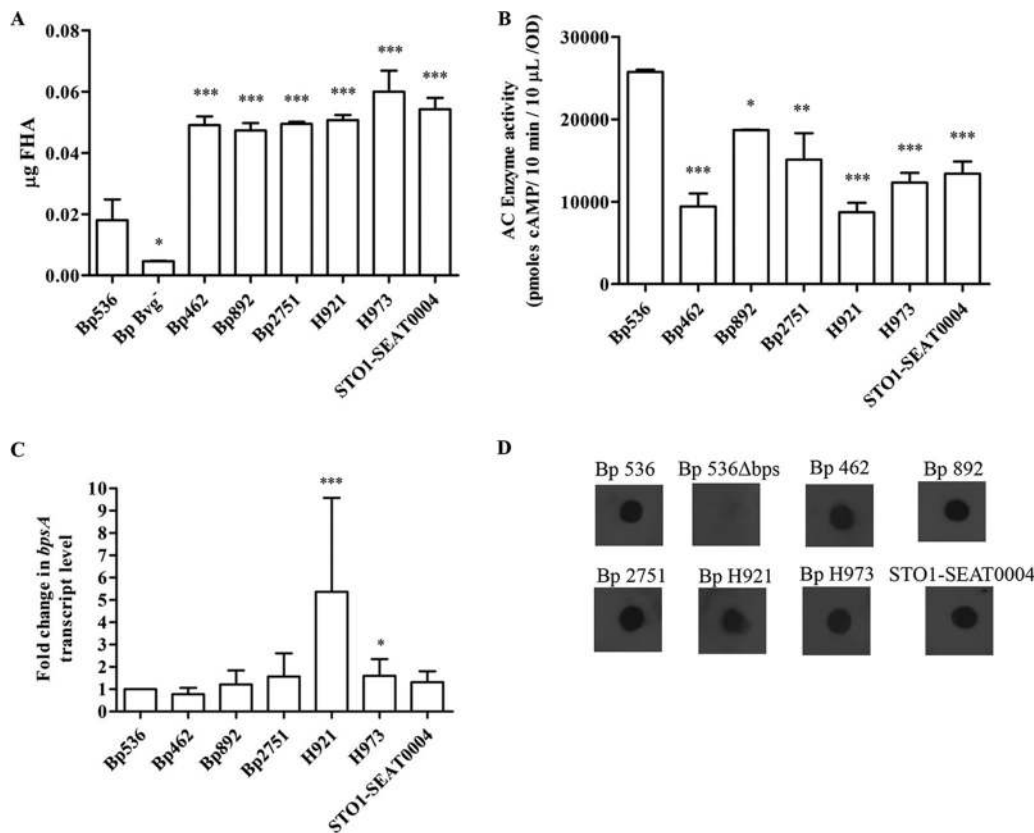


FIG 7 Determination of the levels of biofilm-associated factors/genes in *B. pertussis* strains. (A) Cell surface-associated FHA determination by ELISA. Average values of three replicates are presented with the respective standard deviations. (B) AC toxin activity quantification. AC toxin levels were assessed by enzymatic activity as described earlier (69). (C) *bpsA* expression and production. *bpsA* transcript levels were determined by qPCR and the Pfaffl method. *, $P < 0.05$; **, $P < 0.01$; ***, $P < 0.001$. (D) Dot blot of Bps. Production of Bps was detected as described previously (27).

than did Bp536. However, these differences in cellular attachment levels were statistically significant only for the strains Bp462, H973, and STO1-SEAT0004. As expected, the Bvg⁻ phase-locked strain which does not express FHA and other *Bordetella* adhesins exhibited very low levels of attachment to the epithelial cells.

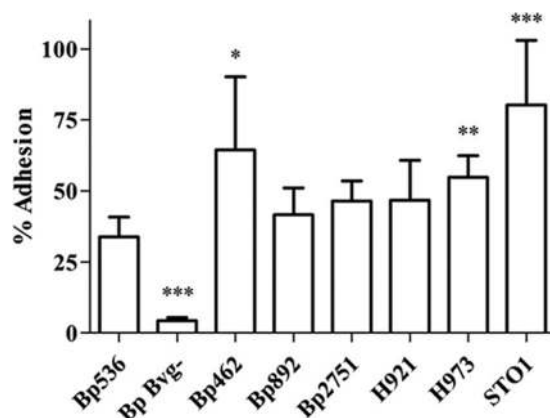


FIG 8 Adherence of *B. pertussis* strains to epithelial cells. Adhesion assays were performed with A549 epithelial cell lines. Each strain was incubated at a multiplicity of infection of 10. Results are expressed as the proportion of adherent bacteria to the amount of the original inoculum. Each data point is the average of three independent experiments performed in duplicate. Error bars indicate the standard deviations. Statistical differences were assessed by one-way ANOVA ($P < 0.0001$) and Student's *t* test with a Bonferroni *post hoc* correction. *, $P < 0.05$; **, $P < 0.01$; ***, $P < 0.001$. Bp Bvg⁻, *B. pertussis* Bvg⁻ phase-locked strain.

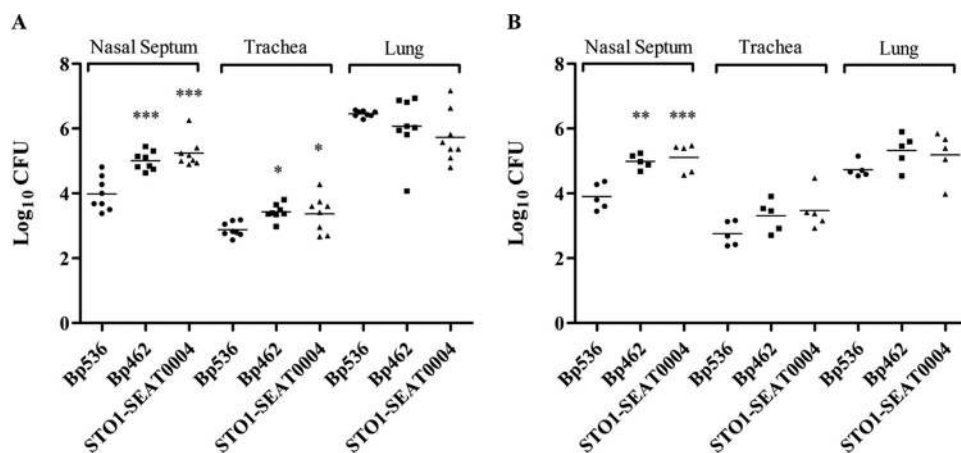


FIG 9 Colonization of mouse respiratory tract by Bp536, Bp462, and STO1-SEA T0004. Groups of C57BL/6 mice were intranasally inoculated with approximately 5×10^5 CFU in $50 \mu\text{l}$ of PBS. At 4 (A) and 7 (B) days postinoculation, animals were sacrificed, and bacterial loads were determined in nasal septum, trachea, and lung. Horizontal bars represent the average values for each group. Significance was analyzed by means of one-way ANOVA and Dunnett's posttest. *, $P < 0.05$; **, $P < 0.01$; ***, $P < 0.001$.

Enhanced colonization of the mouse respiratory tract by recently isolated strains.

To determine the role of a hyperbiofilm phenotype in affecting the outcome of infection, we compared the colonization of Bp536 to the mouse respiratory tract to that of Bp462 and STO1-SEA T0004. Groups of 8- to 10-week-old male and female mice were intranasally inoculated separately with the strains, and the bacterial loads of the nose, trachea, and lungs were determined at 4 and 7 days postinoculation (dpi) (Fig. 9). Consistent with previously published results, high bacterial loads of Bp536 were recovered from all three organs at 4 dpi (Fig. 9A). Compared to Bp536, while the two clinical strains colonized the nose and trachea at high numbers at 4 dpi, no significant differences were found in bacterial numbers harvested from the lungs between any of the strains at this time point. At 7 dpi, all three strains continued to colonize the respiratory organs at high numbers, and the two recent isolates colonized the nose at higher numbers than Bp536 (Fig. 9B). Previously, we have shown the existence of biofilms of *B. pertussis* in the mouse nose and trachea (24, 25, 27) and found that mutants defective in biofilm formation *in vitro* are defective in colonization of the respiratory tract (24, 27). Thus, we propose that the observed hyperbiofilm phenotype of recent isolates contributes to the enhanced respiratory tract colonization.

DISCUSSION

The majority of studies on the biology and pathogenesis of the obligate human pathogen *B. pertussis* have been conducted with the strain BpTohama I and its derivatives. This strain, originally isolated in Japan in the 1950s, is a major source of pertussis vaccines. It has been suggested that it does not represent *B. pertussis* species (14). Although considerable effort is currently being dedicated toward genome sequencing and categorization of genomic differences between circulating clinical strains and domesticated laboratory strains, very little is known regarding their physiological and pathogenic differences. Biofilm formation is considered to be a survival strategy that allows enhanced respiratory tract colonization, persistence, transmission, and circulation of *B. pertussis* in humans (24, 27–29). Characterization of the underlying molecular mechanisms, factors involved, and the assessment of the relationship between biofilms and pathogenesis in currently circulating clinical isolates is important for the development of more effective vaccines and therapeutic alternatives to stem the resurgence of pertussis.

In this study, we utilized *B. pertussis* strains isolated during the period of 2001 to 2012 across two countries, Argentina and the United States. While acellular vaccines are exclusively employed for immunization in the United States, whole-cell vaccines are

used for the first five immunizations, followed by the acellular vaccine as a booster, for 11-year-olds in Argentina. Despite having two different routine pertussis immunization programs, both of these countries have experienced a steady increase in pertussis cases over the last decade. Thus, simultaneous comparison of recently circulating strains from these two countries is likely to shed light not only on variations in microbial pathogenic mechanisms but also on how bacterial pathogens evolve to evade and escape from vaccine-induced immunity.

In comparison to the reference strains, all of the strains, irrespective of the region and the year of isolation, were characterized by hyperbiofilm formation. We propose that hyperbiofilm formation is a highly conserved strategy employed by *B. pertussis* for surface adherence and that this phenotype is maintained independent of the types of vaccines used for immunization.

The mechanisms underlying increased biofilm formation and strain-dependent differences in the biofilm structures of *B. pertussis* were unknown until now. In this report, a positive correlation was found between bacterial hyperaggregation and enhanced biofilm formation in six of the selected currently circulating strains, suggesting that both of these processes depend on the same physical adhesive forces and that these strains may contain similar extracellular matrices that lead to enhanced cell-cell interactions. Structural analyses of biofilms by CLSM revealed significant regional differences in the biofilm architectures. In general, the Argentinean strains formed more compact and regularly shaped biofilms, while the U.S. strains developed distinct microcolonies and more structured and heterogeneous biofilms. The development of complex biofilm architecture has been linked to enhanced antimicrobial properties (44, 45). It remains to be determined if the differences in biofilm architectures between strains from the United States and Argentina are due to bacterial adaptation to dissimilar vaccination programs and if these result in differential resistance to components of host immunity.

FHA and AC toxin have been shown to positively and negatively control biofilm formation in *B. pertussis*, respectively (24, 39). By promoting cell surface and inter-bacterial adhesion, FHA promotes biofilm formation (24). AC toxin inhibits *B. pertussis* biofilm formation by directly interacting with FHA (39). We found an inverse correlation between FHA production and AC toxin activity in recently isolated clinical strains which were characterized by the production of higher levels of FHA and lower AC toxin activity. The observed differences in FHA levels and AC toxin activity could also explain the hyperaggregating property of the clinical strains. FHA is responsible for autoaggregation in *B. pertussis* (46), and autoaggregation in *B. pertussis* is inhibited by addition of AC toxin (39). We propose that by inversely controlling the production of a biofilm-inhibitory and -promoting factor, the clinical strains are able to display higher levels of autoaggregation and biofilm formation. A similar link between production of FHA and AC toxin and hyperbiofilm formation was recently reported by us in a cystic fibrosis isolate of *B. bronchiseptica* which was characterized by higher expression of *phaB* and the absence of the *cyaA* gene from the genome (36). To our knowledge, this report is the first to document the lower AC toxin activity in recently circulating strains of *B. pertussis*. It will be highly informative to determine if this property is conserved in a larger number of strains and in strains isolated from other countries. The observed differences in the levels of FHA and AC toxin activity raise an interesting question regarding the mechanism by which the regulation of these two genes is maintained in the clinical strains.

The *Bordetella bpsABCD* locus required for the synthesis of the Bps polysaccharide is critical for the stability and maintenance of the complex architecture of biofilms (23, 47, 48). Two of the hyperbiofilm formers had higher levels of *bpsA* expression than Bp536, whereas in four others the expression levels of this gene were similar. All of the strains produced Bps. Targeted mutagenesis will offer detailed insights on the relative contributions of individual genes in hyperbiofilm formation of these strains.

A striking result from the present study is the discovery of a link between the hyperbiofilm-forming ability of bacteria and enhanced pathogenic phenotypes. First,

many of the hyperbiofilm-forming strains from both Argentina and the United States exhibited increased adherence to human epithelial cells. The increased cellular adherence of the recently isolated strains is most likely a direct result of enhanced production of FHA. FHA facilitates attachment of *B. pertussis* to a variety of multiple cell types and extracellular structures in the respiratory epithelium (43, 49, 50).

Given the central role that biofilms play in promoting enhanced resistance to chemicals, antimicrobial compounds, and components of host immunity, it is reasonable to hypothesize that a hyperbiofilm phenotype will result in better survival in host tissues and organs. A few studies have directly tested this hypothesis, and the results obtained were generally not supportive. Bacterial mutants that display increased biofilm formation are either equally or significantly less virulent than wild-type strains (51–57). Similarly, while the increased *in vitro* cellular adherence of the hyperbiofilm-forming clinical strains should in theory lead to enhanced colonization in an animal model, previously we did not find this to be the case. A clinical strain of *B. bronchiseptica*, despite exhibiting higher levels of biofilms and epithelial cell adherence than the laboratory strain, was deficient in early colonization of the mouse respiratory tract (36). In this study, two of the recently isolated strains that displayed hyperbiofilm and hyperadherence phenotypes colonized the mouse nose and trachea at higher numbers. Whether the hyperbiofilm-forming ability observed on artificial surfaces and higher bacterial numbers of the clinical strains in mouse nose and trachea correlate with quantitative and qualitative differences in nasal and tracheal biofilms needs to be determined.

In conclusion, we have for the first time demonstrated an association between higher levels of biofilm formation in bacteria with enhanced colonization in an animal model of infection. Based on the data obtained, we propose some mechanistic explanations for the continued circulation of *B. pertussis* and the resurgence of pertussis. Hyperaggregative, hyperbiofilm, and hyperepithelial cell-adhesive properties of the clinical strains most likely result in the formation of robust organ-adherent biofilm communities in the nose and trachea. These biofilm-borne bacteria would survive better in the respiratory tract because of evasion of and escape from immune defenses leading to nasopharyngeal carriage. Droplet or airborne routes are principal ways of *B. pertussis* transmission. Efficient generation and optimal particle size are critical determinates for successful host-host transmission. Droplets are generally defined as being $\geq 5 \mu\text{m}$ size, and droplet sizes at diameters of $30 \mu\text{m}$ or greater can remain suspended in the air. *B. pertussis* is a relatively small bacterium (0.4 to $0.8 \mu\text{m}$) (58). We speculate that increased aggregation of the clinical strains in the respiratory tract could generate optimally sized particles which will resist desiccation during transmission of infectious particles. Thus, a combination of enhanced respiratory tract survival followed by enhanced transmission has led to the resurgence of pertussis. Finally, the conservation of a hyperbiofilm phenotype in *B. pertussis* strains in multiple continents with different vaccine and immunization schedules highlights the urgent need for continued research and development of alternative therapeutics and vaccines targeted toward the biofilm lifestyle.

MATERIALS AND METHODS

Ethics statement. Housing, husbandry, and experiments with animals were carried out in accordance with the guidelines approved by the Institutional Animal Care and Use Committee of Wake Forest School of Medicine. Bacterial strains were collected by regional Microbiology Laboratories in Argentina and at Wake Forest School of Medicine as part of the patients' usual care, without any additional testing for the present investigation. Deidentified organisms were provided to the investigators, and the information received by the investigators was not individually identifiable. The research does not meet the Federal definition of research involving human subject research as outlined in the Code of Federal Regulations (59).

Strains and growth conditions. Strains used in this work are listed in Table 1. Strains S49560 and M3984 were isolated in 2005 at the Wake Forest School of Medicine (WFSM) from a 38-day-old female baby (with coughing spells, apnea events, and cyanosis) and a 7-week-old female baby (with cough and respiratory distress), respectively. Argentinean strains were isolated at La Plata Children's Hospital (Hospital Interzonal de Agudos Especializado en Pediatría Sor María Ludovica), and the patient ages varied between 6 and 16 weeks old. *B. pertussis* strains were maintained on Bordet-Gengou agar (BGA)

TABLE 1 Strains used in this study

Strain	Source or description	Year of isolation (reference)
BpTohama I	Laboratory reference strain	1954
Bp536	Laboratory reference strain, Sm ^r derivative of Tohama I	(72)
Bp369	(Bvg ⁻) derivative of Tohama III	(73)
$\Delta fhaB$ strain	$\Delta fhaB$ mutant	(74)
Δbps strain	Δbps mutant	(27)
Bp462	Argentina	2006
Bp479	Argentina	2007
Bp612	Argentina	2008
Bp892	Argentina	2007
Bp955	Argentina	2001
Bp1938	Argentina	2003
Bp2524	Argentina	2004
Bp2723	Argentina	2001
Bp2751	Argentina	2004
Bp2770	Argentina	2001
H918	USA	2012 (75)
H921	USA	2012 (75)
H973	USA	2012 (75)
H987	USA	2012 (75)
I002	USA	2012 (75)
STO1-CHOC0008	USA	2010 (75)
STO1-SEAT0004	USA	2011 (75)
M3984	USA	2005
S49560	USA	2005

supplemented with 10% (vol/vol) defibrinated sheep blood. For liquid cultures, strains were grown in Stainer-Scholte (SS) broth (35, 60). *Escherichia coli* strains were grown in Luria-Bertani medium. When appropriate, antibiotics were added to maintain plasmids and for strain selection on agar plates: streptomycin, 50 $\mu\text{g ml}^{-1}$; kanamycin, 25 $\mu\text{g ml}^{-1}$; cephalixin, 40 $\mu\text{g ml}^{-1}$.

Biofilm formation assays. For microtiter dish assay of biofilm formation, 100 μl of bacterial suspension prepared at an optical density at 650 nm (OD_{650}) of 1.0 was incubated statically for 4 h at 37°C. After this initial attachment step, medium was carefully removed, fresh SS medium was added, and plates were incubated at 37°C with shaking at 90 rpm. After every 24 h of growth, medium was replaced with fresh SS medium. After the period of incubation indicated in the figures and figure legends, planktonic bacteria were removed, and the OD_{650} was measured. Adhered biomass was quantified by CV staining as previously described (61). Three independent experiments with quadruplicates for each strain were performed.

Autoaggregation assay. Bacteria were cultured in SS medium with heptakis(2,6-di-O-methyl- β -cyclodextrin) and supplement for 24 h (62). Cells were harvested by centrifugation, washed, and resuspended in only SS medium at an OD_{650} of 1.0, followed by static incubation at room temperature. At 2, 5, and 24 h of incubation, 100 μl of the medium was taken out from the top layer of the suspension, and the OD_{650} was measured. The autoaggregation index (AI) was calculated as follows: $(\text{OD}_{t_0} - \text{OD}_t)/\text{OD}_{t_0}$, where OD_{t_0} is the initial OD measurement and OD_t is the OD measured at a designated time point t . Three independent experiments were performed in duplicate for each sample. Statistical significance was evaluated by one-way analysis of variance (ANOVA).

Transformation of *B. pertussis* strains with plasmid pGBSp1-GFP. *B. pertussis* strains were transformed by electroporation (63) of plasmid pGB5P1-GFP (64). Bacterial colonies were selected on BGA containing kanamycin and cultured in SS medium. GFP expression was confirmed by fluorescence microscopy.

Adhesion to abiotic surfaces. GFP-labeled strains were grown overnight in SS medium with kanamycin and used to prepare cell suspensions at an OD_{650} of 0.2. Two milliliters of bacterial suspension was added to individual wells of six-well cell culture plates containing cover glasses (22 by 22 mm), and after 1 h of incubation at 37°C, each well was washed twice with phosphate-buffered saline (PBS). Cover glasses were mounted on glass slides with ProLong Gold antifade reagent (Invitrogen) and observed with a Nikon Eclipse microscope. Adhered cells were counted with the ITCN (image-based tool for counting nuclei) plug-in (65) for ImageJ (66). At least three independent experiments were performed in duplicate for each strain, where four random regions were chosen for bacterial counting.

Structural analysis of biofilms by CLSM. Biofilms were grown on 22- by 22-mm cover glasses in six-well plates in SS medium supplemented with kanamycin. Each well was inoculated with a bacterial suspension at an OD_{650} of 1.0, followed by 4 h of static incubation at 37°C; then the suspensions were removed, and fresh medium was added. After every 24 h of growth, the medium was replaced with fresh SS medium. Cover glasses were washed, mounted as described above, stored at 4°C for 24 h, and visualized with a Nikon Ti-Eclipse confocal microscope. Quantitative data corresponding to structural features of the biofilms were acquired with COMSTAT2 (38). Each experiment was performed at least three times.

TABLE 2 Primer sequences

Primer ^a	Sequence
rpoD-Fw	5'-ATGGGCATCCGCTTCACG
rpoD-Rv	5'-CTTCGTCCAACACCCAC
bpsA-Fw	5'-CGCTGCTGACCATGGATTT
bpsA-Rv	5'-CTGGTGTACAGCATGGTGTGA

^aFw, forward; Rv, reverse.

Enzymatic treatment of biofilms. Biofilms grown in microtiter plates for 96 h were treated with DNase I (40 U) (25), pronase E (1 mg/ml), or sodium metaperiodate (40 mM, pH 5.0) for 2 h at 37°C. Controls were treated with respective reaction buffers: 10 mM Tris-HCl, pH 7.6, 2.5 mM MgCl₂, and 0.5 mM CaCl₂ for DNase I; 10 mM Tris-HCl, pH 7.5, for pronase E; and H₂O for sodium metaperiodate. After each enzymatic treatment, the remaining biofilm was quantified by staining with CV.

ELISA. FHA production was determined by enzyme-linked immunosorbent assay (ELISA) as previously described (67, 68). Briefly, 100 μl of heat-inactivated cells (OD₆₅₀ of 0.05 for FHA) in PBS was added to strip plates (EIA/RIA Stripwell plate; Corning) and incubated overnight at 4°C; cells were washed with PBS buffer containing 0.05% Tween 20 (PBST), followed by blocking with 5% skim milk for 1 h at 37°C. A polyclonal serum raised in mouse (1:20,000 dilution) against purified FHA (Kaketsuken) was used as a primary antibody. Antibody dilutions were prepared in 5% skim milk in PBST. As a control, nonimmune serum was used. After 2 h of incubation at 37°C, plates were washed with PBST, and the secondary antibody (horseradish peroxidase [HRP]-conjugated goat anti-mouse IgG; 1:20,000 dilution) was added, followed by incubation for 2 h at room temperature. After plates were washed with PBST, 100 μl of tetramethyl-benzidine (TMB; Sigma) was added to each well and incubated in the dark for 20 min, followed by addition of 1 M H₂SO₄ to stop the reaction. Absorbance was measured at 450 nm. For FHA protein quantification, a linear standard curve was prepared using different concentrations of purified FHA.

Quantitation of adenylate cyclase enzymatic activity. *B. pertussis* clinical strains were grown to mid-log phase, to an OD₆₅₀ of 0.7 to 0.8. AC activity was determined as previously reported (69).

RNA preparation, cDNA synthesis, and qPCR. *B. pertussis* strains were grown under shaking conditions to an OD₆₅₀ of 1.0, placed immediately on ice, and centrifuged at 4°C, and the bacterial pellets were lysed in RLT buffer (Qiagen). RNA was purified using a Qiagen RNeasy kit and treated with RQ1 DNase I (Promega) for 45 min at 37°C to obtain DNA-free RNA. cDNA was synthesized with random hexamers and SuperScriptIII reverse transcriptase (Invitrogen) as described earlier (70). Differential expression of genes between the strains Bp536, Bp462, Bp892, Bp2751, H921, H973, and STO1-SEAT0004 was analyzed by means of the Pfaffl method (71), following real-time PCR quantification with SYBR green. *rpoD* was used as a housekeeping gene for normalization. Quantitative PCR (qPCR) analysis was performed with three biological and two technical replicates. Primers used for qPCR are listed in Table 2.

Immunoblot analyses. Detection of Bps by immunoblotting was performed as previously described (23, 27). The membrane was probed with a 1:5,000 dilution of a goat antibody raised against *Staphylococcus aureus* poly-*N*-acetyl-β-(1-6)-glucosamine (PNAG) conjugated to diphtheria toxoid. The secondary antibody used was a horseradish peroxidase-conjugated mouse anti-goat immunoglobulin G (IgG) antibody (Pierce) diluted 1:20,000 and detected with an Amersham ECL (enhanced chemiluminescence) Western blotting system.

Bacterial adhesion to epithelial cells. Human alveolar epithelial cells (A549) were cultured at 37°C under 5% CO₂ in Dulbecco's modified Eagle's medium supplemented with 10% fetal bovine serum (FBS) and 4 mM L-glutamine. A549 cells were harvested at 90% confluence, and approximately 2 × 10⁵ cells were seeded in 24-well cell culture plates, followed by incubation overnight. A total of 2 × 10⁶ CFU of *B. pertussis* was added to the wells and centrifuged at 900 rpm for 5 min to facilitate contact between bacteria and epithelial cells; the plates were then incubated at 37°C for 15 min to allow bacterial attachment to A549 cells. The medium was removed, and the wells were washed four times with sterile PBS to remove any nonattached bacteria. The eukaryotic cells were then lysed with 0.05% saponin, and the mixture was plated on BGA containing 10% blood and cephalixin for enumeration of attached bacteria. Adhesion assays were performed in duplicate three times.

Animal experiments. Groups of five to eight 8- to 10-week-old male and female C57BL/6 mice were used for all the experiments. Mice were intranasally inoculated with 50 μl of a bacterial suspension with approximately 5 × 10⁵ CFU of the *B. pertussis* strains indicated in the figures. At 4 days postinfection, mice were sacrificed, and the nasal septum, trachea, and three right lung lobes were harvested. Tissues were homogenized in PBS containing 1% casein and plated on BGA containing 10% blood and streptomycin (for Bp536) or cephalixin (for clinical strains). After 3 to 5 days of growth at 37°C, colonies were enumerated. Statistical significance was determined by one-way ANOVA, and data were determined to be significant at a *P* value of <0.05.

ACKNOWLEDGMENTS

We thank Erik Hewlett and the members of his laboratory for determining the levels of AC toxin and critical reading of the manuscript. Casandra Hoffman, Mary Gray, and Erik Hewlett coordinated the samples, did the assays, and reviewed the data, respectively. We are grateful to Gerry B. Pier for a gift of the PNAG-specific antibody.

This project has been funded in part with federal funds from the National Institute of Allergy and Infectious Diseases, National Institutes of Health, Department of Health and Human Services, under contract numbers HHSN272201200005C, R01AI125560, and 1R21AI123805-01, and with funds from Agencia Nacional de Promoción Científica y Tecnológica (MINCYT, FONCYT, PICT 2012-2514) of Argentina. N.C. was supported by fellowships from CONICET and IUBMB (Wood-Whelan Research Fellowship).

REFERENCES

- Bart MJ, Harris SR, Advani A, Arakawa Y, Bottero D, Bouchez V, Cassiday PK, Chiang CS, Dalby T, Fry NK, Gaillard ME, van Gent M, Guiso N, Hallander HO, Harvill ET, He Q, van der Heide HG, Heuvelman K, Hozbor DF, Kamachi K, Karataev GI, Lan R, Lutynska A, Maharjan RP, Mertsola J, Miyamura T, Octavia S, Preston A, Quail MA, Sintchenko V, Stefanelli P, Tondella ML, Tsang RS, Xu Y, Yao SM, Zhang S, Parkhill J, Mooi FR. 2014. Global population structure and evolution of *Bordetella pertussis* and their relationship with vaccination. *mBio* 5:e01074-14. <https://doi.org/10.1128/mBio.01074-14>.
- Warfel JM, Zimmerman LI, Merkel TJ. 2014. Acellular pertussis vaccines protect against disease but fail to prevent infection and transmission in a nonhuman primate model. *Proc Natl Acad Sci U S A* 111:787-792. <https://doi.org/10.1073/pnas.1314688110>.
- Mooi FR, Van Der Maas NA, De Melker HE. 2014. Pertussis resurgence: waning immunity and pathogen adaptation—two sides of the same coin. *Epidemiol Infect* 142:685-694. <https://doi.org/10.1017/S0950268813000071>.
- Packard ER, Parton R, Coote JG, Fry NK. 2004. Sequence variation and conservation in virulence-related genes of *Bordetella pertussis* isolates from the UK. *J Med Microbiol* 53:355-365. <https://doi.org/10.1099/jmm.0.05515-0>.
- van Amersfoort SC, Schouls LM, van der Heide HG, Advani A, Hallander HO, Bondeson K, von König CH, Riffelmann M, Vahrenholz C, Guiso N, Caro V, Njamkepo E, He Q, Mertsola J, Mooi FR. 2005. Analysis of *Bordetella pertussis* populations in European countries with different vaccination policies. *J Clin Microbiol* 43:2837-2843. <https://doi.org/10.1128/JCM.43.6.2837-2843.2005>.
- Kallonen T, Grondahl-Yli-Hannuksela K, Elomaa A, Lutynska A, Fry NK, Mertsola J, He Q. 2011. Differences in the genomic content of *Bordetella pertussis* isolates before and after introduction of pertussis vaccines in four European countries. *Infect Genet Evol* 11:2034-2042. <https://doi.org/10.1016/j.meegid.2011.09.012>.
- Mooi FR, van Oirschot H, Heuvelman K, van der Heide HG, Gastra W, Willems RJ. 1998. Polymorphism in the *Bordetella pertussis* virulence factors P.69/pertactin and pertussis toxin in The Netherlands: temporal trends and evidence for vaccine-driven evolution. *Infect Immun* 66:670-675.
- van Loo IH, Heuvelman KJ, King AJ, Mooi FR. 2002. Multilocus sequence typing of *Bordetella pertussis* based on surface protein genes. *J Clin Microbiol* 40:1994-2001. <https://doi.org/10.1128/JCM.40.6.1994-2001.2002>.
- Pawloski LC, Queenan AM, Cassiday PK, Lynch AS, Harrison MJ, Shang W, Williams MM, Bowden KE, Burgos-Rivera B, Qin X, Messonnier N, Tondella ML. 2014. Prevalence and molecular characterization of pertactin-deficient *Bordetella pertussis* in the United States. *Clin Vaccine Immunol* 21:119-125. <https://doi.org/10.1128/CVI.00717-13>.
- Hegerle N, Paris AS, Brun D, Dore G, Njamkepo E, Guillot S, Guiso N. 2012. Evolution of French *Bordetella pertussis* and *Bordetella parapertussis* isolates: increase of *Bordetella* not expressing pertactin. *Clin Microbiol Infect* 18:E340-E346. <https://doi.org/10.1111/j.1469-0691.2012.03925.x>.
- Williams MM, Sen K, Weigand MR, Skoff TH, Cunningham VA, Halse TA, Tondella ML. 2016. *Bordetella pertussis* strain lacking pertactin and pertussis toxin. *Emerg Infect Dis* 22:319-322. <https://doi.org/10.3201/eid2202.151332>.
- de Gouw D, Hermans PW, Bootsma HJ, Zomer A, Heuvelman K, Diavatopoulos DA, Mooi FR. 2014. Differentially expressed genes in *Bordetella pertussis* strains belonging to a lineage which recently spread globally. *PLoS One* 9:e84523. <https://doi.org/10.1371/journal.pone.0084523>.
- Mooi FR, van Loo IH, van Gent M, He Q, Bart MJ, Heuvelman KJ, de Greeff SC, Diavatopoulos D, Teunis P, Nagelkerke N, Mertsola J. 2009. *Bordetella pertussis* strains with increased toxin production associated with pertussis resurgence. *Emerg Infect Dis* 15:1206-1213. <https://doi.org/10.3201/eid1508.081511>.
- Caro V, Bouchez V, Guiso N. 2008. Is the sequenced *Bordetella pertussis* strain Tohama I representative of the species? *J Clin Microbiol* 46:2125-2128. <https://doi.org/10.1128/JCM.02484-07>.
- Hall-Stoodley L, Costerton JW, Stoodley P. 2004. Bacterial biofilms: from the natural environment to infectious diseases. *Nat Rev Microbiol* 2:95-108. <https://doi.org/10.1038/nrmicro821>.
- Costerton JW, Cheng KJ, Geesey GG, Ladd TI, Nickel JC, Dasgupta M, Marrie TJ. 1987. Bacterial biofilms in nature and disease. *Annu Rev Microbiol* 41:435-464. <https://doi.org/10.1146/annurev.mi.41.100187.002251>.
- Parsek MR, Singh PK. 2003. Bacterial biofilms: an emerging link to disease pathogenesis. *Annu Rev Microbiol* 57:677-701. <https://doi.org/10.1146/annurev.micro.57.030502.090720>.
- Costerton JW, Stewart PS, Greenberg EP. 1999. Bacterial biofilms: a common cause of persistent infections. *Science* 284:1318-1322. <https://doi.org/10.1126/science.284.5418.1318>.
- Mah TF, O'Toole GA. 2001. Mechanisms of biofilm resistance to antimicrobial agents. *Trends Microbiol* 9:34-39. [https://doi.org/10.1016/S0966-842X\(00\)01913-2](https://doi.org/10.1016/S0966-842X(00)01913-2).
- Donlan RM, Costerton JW. 2002. Biofilms: survival mechanisms of clinically relevant microorganisms. *Clin Microbiol Rev* 15:167-193. <https://doi.org/10.1128/CMR.15.2.167-193.2002>.
- Bosch A, Serra D, Prieto C, Schmitt J, Naumann D, Yantorno O. 2006. Characterization of *Bordetella pertussis* growing as biofilm by chemical analysis and FT-IR spectroscopy. *Appl Microbiol Biotechnol* 71:736-747. <https://doi.org/10.1007/s00253-005-0202-8>.
- Serra D, Bosch A, Russo DM, Rodriguez ME, Zorreguieta A, Schmitt J, Naumann D, Yantorno O. 2007. Continuous nondestructive monitoring of *Bordetella pertussis* biofilms by Fourier transform infrared spectroscopy and other corroborative techniques. *Anal Bioanal Chem* 387:1759-1767. <https://doi.org/10.1007/s00216-006-1079-9>.
- Parise G, Mishra M, Itoh Y, Romeo T, Deora R. 2007. Role of a putative polysaccharide locus in *Bordetella pertussis* development. *J Bacteriol* 189:750-760. <https://doi.org/10.1128/JB.00953-06>.
- Serra DO, Conover MS, Arnal L, Sloan GP, Rodriguez ME, Yantorno OM, Deora R. 2011. FHA-mediated cell-substrate and cell-cell adhesions are critical for *Bordetella pertussis* biofilm formation on abiotic surfaces and in the mouse nose and the trachea. *PLoS One* 6:e28811. <https://doi.org/10.1371/journal.pone.0028811>.
- Conover MS, Mishra M, Deora R. 2011. Extracellular DNA is essential for maintaining *Bordetella pertussis* biofilm integrity on abiotic surfaces and in the upper respiratory tract of mice. *PLoS One* 6:e16861. <https://doi.org/10.1371/journal.pone.0016861>.
- Serra DO, Lucking G, Weiland F, Schulz S, Gorg A, Yantorno OM, Ehling-Schulz M. 2008. Proteome approaches combined with Fourier transform infrared spectroscopy revealed a distinctive biofilm physiology in *Bordetella pertussis*. *Proteomics* 8:4995-5010. <https://doi.org/10.1002/pmic.200800218>.
- Conover MS, Sloan GP, Love CF, Sukumar N, Deora R. 2010. The Bps polysaccharide of *Bordetella pertussis* promotes colonization and biofilm formation in the nose by functioning as an adhesin. *Mol Microbiol* 77:1439-1455. <https://doi.org/10.1111/j.1365-2958.2010.07297.x>.
- Ganguly T, Johnson JB, Kock ND, Parks GD, Deora R. 2014. The *Bordetella pertussis* Bps polysaccharide enhances lung colonization by conferring protection from complement-mediated killing. *Cell Microbiol* 16:1105-1118. <https://doi.org/10.1111/cmi.12264>.
- Cattelan N, Dubey P, Arnal L, Yantorno OM, Deora R. 2016. *Bordetella pertussis* biofilms: a lifestyle leading to persistent infections. *Pathog Dis* 74:ftv108. <https://doi.org/10.1093/femspd/ftv108>.

30. Mallory FB, Hornor AA. 1912. Pertussis: the histological lesion in the respiratory tract. *J Med Res* 27:115–124.3.
31. Paddock CD, Sanden GN, Cherry JD, Gal AA, Langston C, Tatti KM, Wu KH, Goldsmith CS, Greer PW, Montague JL, Eliason MT, Holman RC, Guarner J, Shieh WJ, Zaki SR. 2008. Pathology and pathogenesis of fatal *Bordetella pertussis* infection in infants. *Clin Infect Dis* 47:328–338. <https://doi.org/10.1086/589753>.
32. Soane MC, Jackson A, Maskell D, Allen A, Keig P, Dewar A, Dougan G, Wilson R. 2000. Interaction of *Bordetella pertussis* with human respiratory mucosa in vitro. *Respir Med* 94:791–799. <https://doi.org/10.1053/rmed.2000.0823>.
33. Arnal L, Grunert T, Cattelan N, de Gouw D, Villalba MI, Serra DO, Mooi FR, Ehling-Schulz M, Yantorno OM. 2015. *Bordetella pertussis* isolates from Argentinean whooping cough patients display enhanced biofilm formation capacity compared to Tohama I reference strain. *Front Microbiol* 6:1352. <https://doi.org/10.3389/fmicb.2015.01352>.
34. Dorji D, Graham RM, Richmond P, Keil A, Mukkur TK. 2016. Biofilm forming potential and antimicrobial susceptibility of newly emerged Western Australian *Bordetella pertussis* clinical isolates. *Biofouling* 32:1141–1152. <https://doi.org/10.1080/08927014.2016.1232715>.
35. Mishra M, Parise G, Jackson KD, Wozniak DJ, Deora R. 2005. The BvgAS signal transduction system regulates biofilm development in *Bordetella*. *J Bacteriol* 187:1474–1484. <https://doi.org/10.1128/JB.187.4.1474-1484.2005>.
36. Sukumar N, Nicholson TL, Conover MS, Ganguly T, Deora R. 2014. Comparative analyses of a cystic fibrosis isolate of *Bordetella bronchiseptica* reveal differences in important pathogenic phenotypes. *Infect Immun* 82:1627–1637. <https://doi.org/10.1128/IAI.01453-13>.
37. Silva-Dias A, Miranda IM, Branco J, Monteiro-Soares M, Pina-Vaz C, Rodrigues AG. 2015. Adhesion, biofilm formation, cell surface hydrophobicity, and antifungal planktonic susceptibility: relationship among *Candida* spp. *Front Microbiol* 6:205. <https://doi.org/10.3389/fmicb.2015.00205>.
38. Heydorn A, Nielsen AT, Hentzer M, Sternberg C, Givskov M, Ersboll BK, Molin S. 2000. Quantification of biofilm structures by the novel computer program COMSTAT. *Microbiology* 146:2395–2407. <https://doi.org/10.1099/00221287-146-10-2395>.
39. Hoffman C, Eby J, Gray M, Heath Damron F, Melvin J, Cotter P, Hewlett E. 2017. *Bordetella* adenylate cyclase toxin interacts with filamentous haemagglutinin to inhibit biofilm formation in vitro. *Mol Microbiol* 103:214–228. <https://doi.org/10.1111/mmi.13551>.
40. Scheller EV, Cotter PA. 2015. *Bordetella* filamentous hemagglutinin and fimbriae: critical adhesins with unrealized vaccine potential. *Pathog Dis* 73:ftv079. <https://doi.org/10.1093/femspd/ftv079>.
41. Masin J, Osicka R, Bumba L, Sebo P. 2015. *Bordetella* adenylate cyclase toxin: a unique combination of a pore-forming moiety with a cell-invading adenylate cyclase enzyme. *Pathog Dis* 73:ftv075. <https://doi.org/10.1093/femspd/ftv075>.
42. Villarino Romero R, Osicka R, Sebo P. 2014. Filamentous hemagglutinin of *Bordetella pertussis*: a key adhesin with immunomodulatory properties? *Future Microbiol* 9:1339–1360. <https://doi.org/10.2217/fmb.14.77>.
43. van den Berg BM, Beekhuizen H, Willems RJ, Mooi FR, van Furth R. 1999. Role of *Bordetella pertussis* virulence factors in adherence to epithelial cell lines derived from the human respiratory tract. *Infect Immun* 67:1056–1062.
44. Lewis K. 2005. Persister cells and the riddle of biofilm survival. *Biochemistry (Mosc)* 70:267–274. <https://doi.org/10.1007/s10541-005-0111-6>.
45. Stewart PS, Franklin MJ. 2008. Physiological heterogeneity in biofilms. *Nat Rev Microbiol* 6:199–210. <https://doi.org/10.1038/nrmicro1838>.
46. Menozzi FD, Boucher PE, Riveau G, Gantiez C, Loch C. 1994. Surface-associated filamentous hemagglutinin induces autoagglutination of *Bordetella pertussis*. *Infect Immun* 62:4261–4269.
47. Sloan GP, Love CF, Sukumar N, Mishra M, Deora R. 2007. The *Bordetella* Bps polysaccharide is critical for biofilm development in the mouse respiratory tract. *J Bacteriol* 189:8270–8276. <https://doi.org/10.1128/JB.00785-07>.
48. Nicholson TL, Brockmeier SL, Sukumar N, Paharik AE, Lister JL, Horswill AR, Kehrl ME, Jr, Loving CL, Shore SM, Deora R. 2017. The *Bordetella* Bps polysaccharide is required for biofilm formation and enhances survival in the lower respiratory tract of swine. *Infect Immun* 85:e00261-17. <https://doi.org/10.1128/IAI.00261-17>.
49. Tuomanen E, Weiss A, Rich R, Zak F, Zak O. 1985. Filamentous hemagglutinin and pertussis toxin promote adherence of *Bordetella pertussis* to cilia. *Dev Biol Stand* 61:197–204.
50. Bassinet L, Gueirard P, Maitre B, Housset B, Gounon P, Guiso N. 2000. Role of adhesins and toxins in invasion of human tracheal epithelial cells by *Bordetella pertussis*. *Infect Immun* 68:1934–1941. <https://doi.org/10.1128/IAI.68.4.1934-1941.2000>.
51. Mulcahy H, Lewenza S. 2011. Magnesium limitation is an environmental trigger of the *Pseudomonas aeruginosa* biofilm lifestyle. *PLoS One* 6:e23307. <https://doi.org/10.1371/journal.pone.0023307>.
52. Lin J, Cheng J, Chen K, Guo C, Zhang W, Yang X, Ding W, Ma L, Wang Y, Shen X. 2015. The icmF3 locus is involved in multiple adaptation- and virulence-related characteristics in *Pseudomonas aeruginosa* PAO1. *Front Cell Infect Microbiol* 5:70. <https://doi.org/10.3389/fcimb.2015.00070>.
53. Ha R, Frirdich E, Sychantha D, Biboy J, Taveirne ME, Johnson JG, DiRita VJ, Vollmer W, Clarke AJ, Gaynor EC. 2016. Accumulation of peptidoglycan O-acetylation leads to altered cell wall biochemistry and negatively impacts pathogenesis factors of *Campylobacter jejuni*. *J Biol Chem* 291:22686–22702. <https://doi.org/10.1074/jbc.M116.746404>.
54. de Bentzmann S, Giraud C, Bernard CS, Calderon V, Ewald F, Plesiat P, Nguyen C, Grunwald D, Attree I, Jeannot K, Fauvarque MO, Bordi C. 2012. Unique biofilm signature, drug susceptibility and decreased virulence in *Drosophila* through the *Pseudomonas aeruginosa* two-component system PprAB. *PLoS Pathog* 8:e1003052. <https://doi.org/10.1371/journal.ppat.1003052>.
55. Goodman AL, Kulasekara B, Rietsch A, Boyd D, Smith RS, Lory S. 2004. A signaling network reciprocally regulates genes associated with acute infection and chronic persistence in *Pseudomonas aeruginosa*. *Dev Cell* 7:745–754. <https://doi.org/10.1016/j.devcel.2004.08.020>.
56. Yi X, Yamazaki A, Biddle E, Zeng Q, Yang CH. 2010. Genetic analysis of two phosphodiesterases reveals cyclic diguanylate regulation of virulence factors in *Dickeya dadantii*. *Mol Microbiol* 77:787–800. <https://doi.org/10.1111/j.1365-2958.2010.07246.x>.
57. Candon HL, Allan BJ, Fraley CD, Gaynor EC. 2007. Polyphosphate kinase 1 is a pathogenesis determinant in *Campylobacter jejuni*. *J Bacteriol* 189:8099–8108. <https://doi.org/10.1128/JB.01037-07>.
58. Gralton J, Tovey E, McLaws ML, Rawlinson WD. 2011. The role of particle size in aerosolised pathogen transmission: a review. *J Infect* 62:1–13. <https://doi.org/10.1016/j.jinf.2010.11.010>.
59. Code of Federal Regulations. 2009. Title 45. Public welfare. Department of Health and Human Services, part 46. Protection of human subjects. 45 CFR 46. U.S. Government Printing Office, Washington, DC.
60. Sukumar N, Sloan GP, Conover MS, Love CF, Mattoo S, Kock ND, Deora R. 2010. Cross-species protection mediated by a *Bordetella bronchiseptica* strain lacking antigenic homologs present in acellular pertussis vaccines. *Infect Immun* 78:2008–2016. <https://doi.org/10.1128/IAI.01142-09>.
61. Merritt JH, Kadouri DE, O'Toole GA. 2005. Growing and analyzing static biofilms. *Curr Protoc Microbiol* Chapter 1:Unit 1B1. <https://doi.org/10.1002/9780471729259.mc01b01s00>.
62. Stainer DW, Scholte MJ. 1970. A simple chemically defined medium for the production of phase I *Bordetella pertussis*. *J Gen Microbiol* 63:211–220. <https://doi.org/10.1099/00221287-63-2-211>.
63. Zealey GR, Yacoob RK. 2000. Electrotransformation of *Bordetella*, p 150–156. In Eynard N, Teissie J (ed), *Electrotransformation of bacteria*. Springer, Berlin, Germany.
64. Weingart CL, Broitman-Maduro G, Dean G, Newman S, Peppler M, Weiss AA. 1999. Fluorescent labels influence phagocytosis of *Bordetella pertussis* by human neutrophils. *Infect Immun* 67:4264–4267.
65. Byun J, Verardo MR, Sumengen B, Lewis GP, Manjunath BS, Fisher SK. 2006. Automated tool for the detection of cell nuclei in digital microscopic images: application to retinal images. *Mol Vis* 12:949–960.
66. Schneider CA, Rasband WS, Eliceiri KW. 2012. NIH Image to ImageJ: 25 years of image analysis. *Nat Methods* 9:671–675. <https://doi.org/10.1038/nmeth.2089>.
67. Barkoff AM, Guiso N, Guillot S, Xing D, Markey K, Berbers G, Mertsola J, He Q. 2014. A rapid ELISA-based method for screening *Bordetella pertussis* strain production of antigens included in current acellular pertussis vaccines. *J Immunol Methods* 408:142–148. <https://doi.org/10.1016/j.jim.2014.06.001>.
68. Tsang RS, Sill ML, Advani A, Xing D, Newland P, Hallander H. 2005. Use of monoclonal antibodies to serotype *Bordetella pertussis* isolates: comparison of results obtained by indirect whole-cell enzyme-linked immunosorbent assay and bacterial microagglutination methods. *J Clin Microbiol* 43:2449–2451. <https://doi.org/10.1128/JCM.43.5.2449-2451.2005>.
69. Eby JC, Gray MC, Warfel JM, Paddock CD, Jones TF, Day SR, Bowden J, Poulter MD, Donato GM, Merkel TJ, Hewlett EL. 2013. Quantification of

- the adenylate cyclase toxin of *Bordetella pertussis* in vitro and during respiratory infection. *Infect Immun* 81:1390–1398. <https://doi.org/10.1128/IAI.00110-13>.
70. Conover MS, Redfern CJ, Ganguly T, Sukumar N, Sloan G, Mishra M, Deora R. 2012. BpsR modulates *Bordetella* biofilm formation by negatively regulating the expression of the Bps polysaccharide. *J Bacteriol* 194:233–242. <https://doi.org/10.1128/JB.06020-11>.
71. Pfaffl MW. 2001. A new mathematical model for relative quantification in real-time RT-PCR. *Nucleic Acids Res* 29:e45. <https://doi.org/10.1093/nar/29.9.e45>.
72. Stibitz S, Yang MS. 1991. Subcellular localization and immunological detection of proteins encoded by the vir locus of *Bordetella pertussis*. *J Bacteriol* 173:4288–4296. <https://doi.org/10.1128/jb.173.14.4288-4296.1991>.
73. Weiss AA, Falkow S. 1984. Genetic analysis of phase change in *Bordetella pertussis*. *Infect Immun* 43:263–269.
74. Carbonetti NH, Artamonova GV, Andreasen C, Dudley E, Mays RM, Worthington ZE. 2004. Suppression of serum antibody responses by pertussis toxin after respiratory tract colonization by *Bordetella pertussis* and identification of an immunodominant lipoprotein. *Infect Immun* 72:3350–3358. <https://doi.org/10.1128/IAI.72.6.3350-3358.2004>.
75. Harvill ET, Goodfield LL, Ivanov Y, Meyer JA, Newth C, Cassidy P, Tondella ML, Liao P, Zimmerman J, Meert K, Wessel D, Berger J, Dean JM, Holubkov R, Burr J, Liu T, Brinkac L, Kim M, Losada L. 2013. Genome sequences of 28 *Bordetella pertussis* U.S. outbreak strains dating from 2010 to 2012. *Genome Announc* 1:e01075-13. <https://doi.org/10.1128/genomeA.01075-13>.